The Microwave Spectrum and Molecular Conformation of Peroxynitric Acid (HOONO2)

ARTICLE *in* JOURNAL OF MOLECULAR SPECTROSCOPY · APRIL 1986

Impact Factor: 1.48 · DOI: 10.1016/0022-2852(86)90136-0

JOURNAL OF MOLECULAR SPECTROSCOPY 116, 406–421 (1986)

The Microwave Spectrum and Molecular Conformation of Peroxynitric Acid ($HOONO_2$)

R. D. SUENRAM AND F. J. LOVAS

Molecular Spectroscopy Division, National Bureau of Standards, Gaithersburg, Maryland 20899

AND

H. M. PICKETT

Jet Propulsion Laboratory, California Institute of Technology, Pasadena, California 91109

The rotational spectrum of peroxynitric acid has been investigated in the 40- to 120-GHz region. The spectrum of the ground state is complicated by tunneling of the OH group, which causes a doubling of the asymmetric rotor spectrum. The magnitude of the tunneling splitting is such that it causes Coriolis interactions between the energy levels of the two tunneling states which lead to perturbations in the rotational spectrum. A combined analysis of the *a*- and *b*-type pure rotational transitions with the *c*-type tunneling transitions allows a perturbation-free determination of the rotational constants for the ground state. A similar analysis of the low-lying NO_2 torsional vibration at 145(6) cm^{-1} has also been carried out. The dipole moments for each state have been determined by analysis of the second-order Stark effect. The molecular structure analysis indicates that all the heavy atoms are planar and only the hydrogen atom is out of the heavy atom plane. The preferred orientation of the hydrogen atom with respect to the plane of the heavy atoms is at an angle of $\sim 106°$ with respect to the *cis* conformation.

I. INTRODUCTION

As part of our continuing effort to provide accurate microwave spectroscopic information about molecules of atmospheric interest, we have studied the microwave spectrum of peroxynitric acid ($HOONO_2$; see Fig. 1). Previous papers in this series have dealt with the microwave spectra of hypochlorous acid (HOCl) and chlorine nitrate ($ClNO_3$) (*1, 2*).

Peroxynitric acid was first discovered in 1977 by Niki *et al.* (*3*) in the reaction of nitrogen dioxide with the HOO radical. Niki *et al.* detected it by observing and recording its infrared spectrum. Since then, numerous kinetic studies have been carried out (*4–8*) which provide a wealth of information about its reaction rates and importance in atmospheric chemistry.

To date, there has been no direct detection of $HOONO_2$ in the atmosphere. These efforts are seriously hampered by the lack of any high-resolution spectral data for the molecule. The observation and analysis of the microwave spectrum should lay the ground work for further high-resolution studies in the far-infrared and infrared regions.

0022-2852/86 $3.00

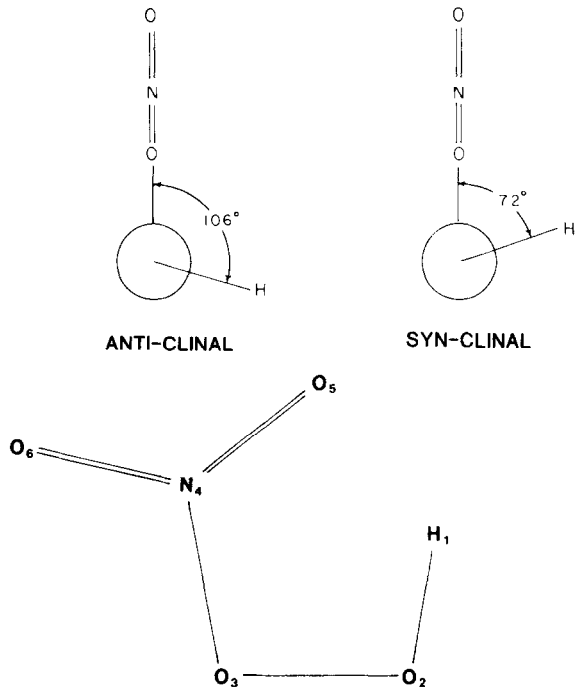

FIG. 1. The *syn*-clinal and *anti*-clinal forms of peroxynitric acid as well as the atom numbering scheme used throughout the paper.

II. EXPERIMENTAL DETAILS

(a) Sample Preparation

Fresh samples of peroxynitric acid were prepared on a daily basis following the method of Kenley *et al.* (*7*). This method involves the sequential addition of small amounts of NO_2BF_4 (0.4 g total) to an excess of 90% HOOH (2 g total) which was magnetically stirred and cooled to 0°C in an ice bath. A slow stream of Ar was used to continuously flush the sample since the addition of solid NO_2BF_4 is accompanied by vigorous effervescence of brown gas. Anyone who is planning to prepare samples of peroxynitric acid should read the precautions put forth in the original paper [Ref. (*7*)] before attempting its synthesis. Following the preparation, the sample of $HOONO_2$ in HOOH was transferred via pipet to a sample vial which was attached directly to the sample inlet of the spectrometer. The sample was cooled with an ice bath and the vapor from the sample was then allowed to flow continuously through the absorption cell. This preparation proved fairly convenient and provided a reliable source of $HOONO_2$ in the absorption cell. The intensity of the microwave lines from samples prepared in this fashion were about 10 times stronger than could be obtained from a second method which involved the addition of 90% HOOH to a sample of HNO_3 (*7*). This second synthesis also leaves a fairly large residual amount of HNO_3 in the reaction mixture which introduced a large number of interfering lines. With the first synthesis, nitric acid lines were observed to be very weak in the vapor from the sample.

(b) Spectrometer and Operating Conditions

The spectrometer employed was of conventional design with 80-kHz square wave Stark modulation (*9*). Transition frequencies were measured under computer control with each measurement being the result of at least one up–down pair of frequency scans. The frequencies of all transitions, which could be fully modulated, were determined using a Gauss fitting routine which yields accurate line peak positions.

Two absorption cells were used during the course of this work. For frequency measurements in the 80- to 120-GHz range, a 30-cm-long parallel plate cell was used, with aluminum plates and a glass vacuum envelope. Measurements below 80 GHz were made in a 1-m-long parallel plate cell with stainless steel plates inside a glass vacuum envelope. Details of the construction of both cells have been previously published (*10*).

In a typical experiment, vapor from the sample reservoir was flowed through the cell on a continuous basis with the pressure in the cell being maintained at 15–30 mTorr (~1–2 Pa) of mercury. The linewidth of the transitions under these conditions was approximately 0.3 MHz.

III. SPECTRAL ASSIGNMENTS

In order to obtain initial spectral predictions for peroxynitric acid, structures of nitric acid and hydrogen peroxide (see Table I), minus an H atom, were combined to yield estimates for the structural parameters. The most uncertain of the bond lengths and angles in these estimates were felt to be the N–O bond length and the N–O–O angle, since this is where the two subunits join. A more difficult aspect of the structure estimates was estimating which conformer, of the many that are possible, would be the one of lowest energy. From previous work, nitric acid (*11*), methyl nitrate (*12*), and ethyl nitrate (*13*) are known to have planar heavy atom structures while hydrogen peroxide is *gauche* with a dihedral angle of ~120° between the HOO planes (*14*). Peroxyformic and peroxyacetic acids have both been studied by microwave techniques (*15, 16*). Both of these species exhibit a planar heavy atom structure, like the nitrates, as well as having a planar OH group. This planarity is partially due to the ability of the peroxyacid part of the molecule to form an internal hydrogen bond. Starting from

TABLE I

Structural Parameters from HNO_3 and HOOH[a]

HNO_3 from Reference #11	HOOH from Reference #14
$r(N_4 - O_3)$ = 1.396	r(O - H) = 0.965
$r(N_4 - O_5)$ = 1.226	r(O - O) = 1.464
$r(N_4 - O_6)$ = 1.196	∠HOO = 99.4
$\angle O_3N_4O_5$ = 115.8	dihedral angle = 120.7
$\angle O_3N_4O_6$ = 115.2	

[a]Bond lengths in Angstroms and angles in degrees.

our initial estimates, the N–O–O and O–O–H angles and the dihedral angle between the NO_2 and HO_2 planes were varied to yield parameters for the *cis*-planar, *trans*-planar, peroxide-like (*anti*-clinal), and various other conformers. Most of these predictions resulted in similar rotational constants with $A = \sim 12.6$ GHz, $B = \sim 4.7$ GHz, and $C = \sim 3.4$ GHz. This meant that all conformers would exhibit a spectrum of a prolate rotor. Furthermore, all of the conformers considered had nonzero estimated values for the μ_a component of the dipole moment. For such a species, the strong *a*-type *R*-branch transitions of intermediate to high K_{-1} will occur in clusters in the regions of integral multiples of $B + C$. Thus, regardless of the conformation, it was anticipated that by searching at least 8 GHz, one of these cluster regions would be observed. Starting at 110 GHz and searching to higher frequency, a dense cluster of transitions around 115 GHz was found. Assuming this was one of the *a*-type *R*-branch clusters, a search in the vicinity of 107 GHz was carried out and again a spectrally dense region was found. By taking frequency differences between lines in the two regions, these transitions could be assigned to the $J = 14$–13 and $J = 13$–12 *a*-type *R*-branch clusters, respectively. Some trial and error fitting of alternate K values eventually led to full quantum number assignment. After the *a*-type transitions had been assigned and fitted, *b*-type and *c*-type transitions were sought in their predicted regions. The *b*-type transitions were readily found but *c*-type lines were absent.

For a simple asymmetric rotor spectrum this would have completed the assignment but as is seen in Fig. 2, each high-K_{-1} *a*-type *R*-branch line appeared as an asymmet-

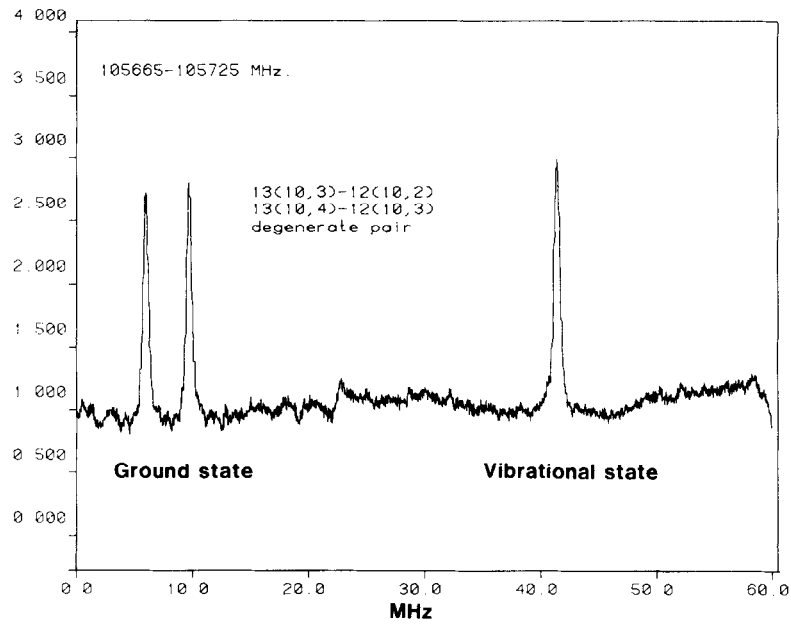

FIG. 2. The typical spectral pattern that was observed for high-K_{-1} transitions. The left pair is the degenerate pair of transitions indicated which are split by the hydroxyl tunneling. The transition on the right is the corresponding degenerate pair of transitions for the NO_2 torsion, only now the magnitude of the splitting induced by the hydroxyl tunneling is not large enough to be observed.

rically spaced equally intense triplet. This unusual splitting complicated the assignment since such splittings are difficult to rationalize for a species with a singlet ground state electronic configuration. Several phenomena were considered which could give rise to spectral splittings of the nature observed. The first situation considered was a tunneling motion of the hydrogen between two equivalent conformations similar to the tunneling in hydrogen peroxide. This tunneling, however, would give rise to a doublet structure. The second possibility considered was that the ground state transitions are split into a doublet by tunneling (the closely spaced doublet) and the remaining transition is only one-half of the first excited OH torsional state transition which is split by a larger amount by the tunneling of the hydroxyl hydrogen. Extensive searching for the missing half of this type of transition proved fruitless. Furthermore, since the intensity of the "singlet" was equal to the intensity of each of the "doublets," this would require that the OH torsion be very low in energy (<50 cm^{-1}). This seemed unreasonable since the lowest vibrational mode expected would be the O–NO_2 torsion which should be in the 100- to 200-cm^{-1} range based on correlations with similar molecules. For fluorine nitrate this mode occurs at 152 cm^{-1} (*17*) and in methyl nitrate it occurs at 130 cm^{-1} (*12*). A vibrational energy of this magnitude would give transition intensities about one-half the intensity of the ground state. Thus, this hypothesis seemed in error and we considered the possibility that the "singlet" was actually a near degenerate doublet. Subsequently, a careful analysis of the 7_{07}–6_{06} transition at low and high Stark voltage revealed that it was a very closely spaced doublet. Further work on other transitions showed that they also had a doublet structure. In summary, what we have observed is a ground state transition and a low-lying vibrational state which is the NO_2 torsion. Both states are split by the OH torsion, the ground state by ~5–10 MHz, and the vibrational state by <1 MHz. The implications of these observations are discussed below.

IV. PERTURBATIONS AND THE TUNNELING MOTION

In addition to the doubling of the spectral lines due to proton tunneling, some of the transitions of the ground state were found to be perturbed from their normal asymmetric rotor frequencies. This is caused by a Coriolis interaction between near degenerate rotational levels of the lower and upper tunneling states. Noting the direction and magnitude of these shifts, which should be equal and opposite in sign for the two interacting tunneling states, it was possible to determine that the energy difference must be in the range of 0.04–0.06 cm^{-1} between the tunneling states. Since the splitting in $v = 1$ of the NO_2 torsion was much smaller, a lower energy difference was expected. Using this information, estimates of the frequencies of the *c*-type tunneling transitions were obtained for both the ground and first excited state of the NO_2 torsion. These transitions were then sought and easily found.

Most of the spectral fitting was carried out using a centrifugal distortion Hamiltonian of the Watson type (*18*) and a computer program written by Kirchhoff (*19*). Due to the perturbations caused by the tunneling motion, this basic Hamiltonian is inadequate. Thus, we turned to the Hamiltonian developed by Pickett (*20*):

$$H_v = [A - \tfrac{1}{2}(B + C)]P_z^2 + \tfrac{1}{2}(B + C)P^2 + \tfrac{1}{2}(B - C)(P_x^2 - P_y^2) - D_J P^4 - D_{JK} P_z^2 P^2 - D_K P_z^4 - 2\delta_J P^2(P_x^2 - P_y^2) - \delta_K[P_z^2(P_x^2 - P_y^2) + (P_x^2 - P_y^2)P_z^2] + E_v + H_{12} \quad (1)$$

which allows a simultaneous fitting of the normal asymmetric rotor centrifugal distortion terms with the *c*-type Coriolis interaction included. The Coriolis term used here is of the form

$$H_{12} = F_{bc}(P_bP_c + P_cP_b). \tag{2}$$

This type of term, which couples the two tunneling states, is not strictly appropriate for a periodic torsional coordinate (*20*). However, if the potential has a very high barrier, in addition to the tunneling barrier, the tunneling potential can be approximated as a simple double minimum potential in an aperiodic coordinate. With this assumption, Eq. (2) is appropriate although, by symmetry, F_{ac} is also allowed. The perturbations due to this term, however, were correlated with the centrifugal distortion constants and, therefore, F_{ac} was fixed at zero.

The observed transitions and results of the final fit of all the observed *a*- and *b*-type pure rotational transitions are given in Table II for the ground state and Table III for the NO_2 torsion. The *c*-type transitions between inversion doublets ($v = 0$ and $v = 1$) for the ground and vibrational state are combined in Table IV. The resulting constants are presented in Table V.

V. STRUCTURE

Since only one isotopic species has been investigated, a precise structural determination is not possible. However, certain aspects of the overall conformation are readily apparent. From the small nonplanar moment $2P_{cc} = I_c - I_b - I_a = 1.70\ \mu A^2$, it is evident that either (a) all the heavy atoms must lie in a plane with the proton out of the plane, or (b) the proton is in the *cis*- or *trans*-planar configuration and all of the other atoms lie within <0.1 A of the planar configuration, but not planar. Since tunneling is observed and symmetry must be maintained in this motion, the most logical explanation is that the heavy atoms lie in a plane with the hydrogen atom inverting symmetrically about this plane to provide equivalent conformations. This must be true for both the ground state and the vibrational state. This means that the overall geometry must be *gauche*. With only the rotational constant data it is difficult to determine if the *gauche* form is *anti*-clinal (like hydrogen peroxide) or whether it is *syn*-clinal which would put it half way between the *cis*-planar nitrate molecules and the *anti*-clinal hydrogen peroxide species (*21*).

Since the three rotational constants are independent, we can use these to determine three structural parameters in the molecule in an r_0 structural fit. The three parameters which are most in question are the N–O bond length, the N–O–O angle, and the dihedral angle (τ) between the NO_2 group and the hydrogen atom. All of the other parameters in the molecule were fixed at their nitric acid or hydrogen peroxide values (see Table I) and these three parameters were fitted using Schwendeman's STRFIT program (*22*). From the results of this fit it became apparent that it was possible to obtain realistic fits for both a *syn*-clinal and an *anti*-clinal form. For the *syn*-clinal form the resulting parameters are $r(NO) = 1.511$ A, $\angle NOO = 102.9°$, and $\tau = 72.8°$, respectively. For the *anti*-clinal form, the corresponding parameters are 1.515 A, 101.2°, and 106.2°. It should be emphasized that the assumptions described above went into the calculations and therefore the resulting parameters may not have the usual degree of accuracy. Nonetheless, it is interesting that both fits yield approximately the same

TABLE II

Observed *a*-Type and *b*-Type Rotational Transitions for $HOONO_2$ in the $v = 0$ and $v = 1$ Tunneling States of the Ground Vibrational State (in MHz)

Transition	Measured Frequency v=0	Obs.-Calc.	Measured Frequency v=1	Obs.-Calc.
5(3, 3) - 4(3, 2)	40722.050(70)a	-0.029	40720.800(70)a	0.000
5(3, 2) - 4(3, 1)	40951.450(40)	-0.008	40950.160(40)	0.029
7(1, 7) - 6(1, 6)	50604.000(100)	-0.011		
7(0, 7) - 6(0, 6)	51171.790(100)	0.007	51170.670(50)	-0.130
6(2, 4) - 5(2, 3)	51543.270(100)	-0.016	51541.580(100)	-0.003
7(2, 6) - 6(2, 5)	55289.420(100)	-0.011	55287.850(100)	-0.010
7(3, 5) - 6(3, 4)	57096.300(50)	-0.018		
7(4, 4) - 6(4, 3)	57154.840(40)	0.009	57152.730(40)	0.005
7(4, 3) - 6(4, 2)	57235.440(40)	-0.010	57233.330(40)	0.005
7(3, 4) - 6(3, 3)	58368.000(100)	0.159	58338.200(40)	-0.003
11(0,11) - 10(0,10)	78072.300(100)	-0.062	78071.170(100)	0.043
11(1,11) - 10(0,10)			78133.250(40)	0.015
10(8, 3) - 9(8, 2)	81265.990(100)	-0.030	81263.190(70)	0.043
10(8, 2) - 9(8, 1)	81265.990(100)	-0.030	81263.190(70)	0.042
10(7, 4) - 9(7, 3)	81394.053(44)*	-0.002	81391.136(41)*	0.014
10(7, 3) - 9(7, 2)	81394.053(44)*	-0.058	81391.136(41)*	-0.042
10(6, 5) - 9(6, 4)			81589.812(44)	0.053
10(6, 4) - 9(6, 3)	81595.450(43)	-0.026		
10(5, 6) - 9(5, 5)	81902.815(51)	0.017	81899.719(49)	0.019
10(5, 5) - 9(5, 4)	81975.613(47)	-0.018	81972.511(48)	-0.005
10(4, 7) - 9(4, 6)	82134.500(50)	0.014		
10(4, 6) - 9(4, 5)			83139.884(43)	0.039
12(11, 1) - 11(11, 0)	97390.000(80)	-0.014	97386.610(100)	-0.042
12(10, 2) - 11(10, 1)	97470.550(90)	-0.036	97467.150(90)	-0.032
12(9, 3) - 11(9, 2)	97578.720(70)	0.036	97575.250(70)	0.023
12(8, 5) - 11(8, 4)	97729.778(55)	0.044	97726.226(55)	0.020
12(7, 6) - 11(7, 5)	97951.715(60)	0.028	97948.150(60)	0.093
12(7, 5) - 11(7, 4)	97952.515(65)	-0.012	97948.850(60)	-0.046
12(6, 7) - 11(6, 6)	98292.276(62)	-0.019	98288.520(62)	0.004
12(6, 6) - 11(6, 5)	98315.770(60)	-0.003	98311.877(57)	-0.112
14(0,14) - 13(1,13)	98401.560(31)	-0.007	98400.054(41)	-0.056
14(1,14) - 13(1,13)	98409.522(32)	-0.016	98408.057(33)	-0.024
14(0,14) - 13(0,13)	98417.520(40)	-0.013	98416.050(30)	-0.026
14(1,14) - 13(0,13)	98425.500(30)	-0.004	98424.050(40)	0.003
12(5, 8) - 11(5, 7)	98737.640(160)*	-0.560	98737.640(160)*	0.235
12(5, 7) - 11(5, 6)	99120.500(200)*	-0.352	99120.500(200)*	0.532
10(7, 3) - 10(6, 4)	102663.100(90)*	-0.240	102663.100(90)*	0.159
10(7, 4) - 10(6, 5)	102666.720(90)*	-0.152	102666.720(90)*	0.247
8(7, 1) - 8(6, 2)	103010.130(60)*	-0.203	103010.130(60)*	0.357
8(7, 2) - 8(6, 3)			103010.130(60)*	0.175
7(7, 1) - 7(6, 2)	103112.050(60)*	-0.308	103112.050(60)*	0.300
7(7, 0)*- 7(6, 1)	103112.050(60)*	-0.282	103112.050(60)*	0.326
14(2,13) - 13(2,12)	104985.020(30)	-0.049		
15(0,15) - 14(1,14)	105198.173(29)	0.002	105196.660(26)	0.023
15(1,15) - 14(1,14)	105202.100(36)	-0.018	105200.575(33)	-0.009
15(0,15) - 14(0,14)	105206.113(34)	-0.029	105204.595(34)	-0.014
15(1,15) - 14(0,14)	105210.073(30)	-0.016	105208.567(26)	0.012
14(1,13) - 13(1,12)			105228.303(40)	-0.018
13(12, 2) - 12(12, 1)	105494.410(50)	0.016	105490.780(60)	0.009
13(11, 2) - 12(11, 1)	105572.760(50)	0.001	105569.100(50)	0.006
13(10, 4) - 12(10, 3)	105674.750(50)	0.030	105671.020(50)	0.016
13(9, 4) - 12(9, 3)	105811.910(60)	0.004	105808.140(60)	0.017
13(8, 6) - 12(8, 5)	106004.242(50)	0.059	106000.356(50)	0.044
13(7, 7) - 12(7, 6)	106287.310(50)	-0.016	106283.320(50)	-0.004
13(7, 6) - 12(7, 5)	106289.930(50)	-0.012	106285.930(50)	-0.010
13(6, 8) - 12(6, 7)	106713.722(46)	-0.005	106709.611(53)	0.008
13(6, 7) - 12(6, 6)	106772.270(200)	-0.115	106768.242(53)	-0.008
13(5, 9) - 12(5, 8)	107184.570(50)	0.024	107217.140(60)	-0.032
13(5, 8) - 12(5, 7)	107919.050(50)	0.022	107951.530(60)	0.048
14(3,12) - 13(3,11)	110936.550(50)	-0.125		
16(0,16) - 15(1,15)			111990.150(100)*	-0.020
16(1,16) - 15(1,15)	111993.760(40)	0.037	111992.100(40)	-0.011
16(0,16) - 15(0,15)	111995.750(50)*	0.021	111994.110(40)	-0.007
16(1,16) - 15(0,15)	111997.700(100)	0.030	111995.750(50)	-0.308
14(12, 3) - 13(12, 2)	113674.320(50)	-0.004	113670.380(50)	-0.022

a) Uncertainties refer to the last digits given. An asterisk after the frequency indicates blended lines. See the text for a discussion of the fitting of these blends.

TABLE II—*Continued*

Transition	Measured Frequency v=0	Obs.-Calc.	Measured Frequency v=1	Obs.-Calc.
14(12, 2) - 13(12, 1)	113674.320(50)	-0.004	113670.380(50)	-0.022
14(10, 5) - 13(10, 4)	113898.600(40)	-0.007	113894.550(40)	-0.022
14(9, 5) - 13(9, 4)	114069.891(37)	-0.014	114065.779(36)	-0.010
14(8, 7) - 13(8, 6)	114310.889(57)*	0.153	114306.655(59)*	0.147
14(8, 6) - 13(8, 5)	114310.889(57)*	-0.102	114306.655(59)*	-0.110
22(3,19) - 22(2,20)	114423.310(40)	-0.030		
14(7, 8) - 13(7, 7)	114665.549(45)	-0.017	114661.192(42)	0.015
14(7, 7) - 13(7, 6)	114672.855(48)	-0.036	114668.483(45)	-0.018
18(8,10) - 18(7,11)	115061.740(40)	0.066	115060.540(40)	-0.037
22(4,19) - 22(3,20)	115159.890(60)	0.057	115143.670(80)	0.096
14(6, 9) - 13(6, 8)	115181.810(60)	0.023	115177.660(60)	0.040
14(6, 8) - 13(6, 7)	115315.982(55)	0.011	115311.802(53)	0.031
14(5,10) - 13(5, 9)	115614.970(50)	-0.038	115536.320(60)	-0.059
14(5, 9) - 13(5, 8)	117106.790(45)	0.106	117027.770(60)	0.020
13(8, 5) - 13(7, 6)	118085.710(100)*	-0.227	118085.710(100)*	0.039
13(8, 6) - 13(7, 7)	118089.540(100)*	-0.060	118089.540(100)*	0.207
11(8, 3) - 11(7, 4)	118594.280(100)*	-0.115	118594.280(100)*	0.384
11(8, 4) - 11(7, 5)	118594.280(100)*	-0.415	118594.280(100)*	0.084
10(8, 3) - 10(7, 4)	118765.230(30)*	-0.022	118764.650(30)*	-0.023
10(8, 2) - 10(7, 3)	118765.230(30)*	0.046	118764.650(30)*	0.044
17(0,17) - 16(1,16)	118783.960(50)*	0.170	118782.130(50)	0.032
16(2,15) - 15(1,14)			118782.650(100)	0.062
17(1,17) - 16(1,16)	118784.710(100)	-0.028	118783.030(50)	-0.016
17(0,17) - 16(0,16)	118785.700(50)	-0.031	118783.960(50)*	-0.078
17(1,17) - 16(0,16)	118786.640(50)	-0.038		

values for the N–O bond and the N–O–O angle and only the dihedral angle remains in question. The dipole moment analysis, described in the next section, provides more information on the structure.

The structural information derived above can be used to predict the value of F_{bc} using the analysis of Pickett (*20*). Following the notation of Pickett (*20*), C_a is calculated in the inertial axis system using finite differences to obtain the derivatives of the atomic coordinates with respect to torsion. The value of C_a obtained is to a good approximation equal to $(1 - \cos 2\tau) \times 0.01364/\text{rad}$, where τ = the torsional angle. The integral of $-C_a$ is equal to the rotation angle, θ_R, relating the reduced axes to the principal axes. Integration of $-C_a$ from $\tau = 0$ to 72.8° yields −0.0134 while integration of $-C_a$ from $\tau = 180$ to 106.2° yields +0.0139. These integrals yield θ_R of −0.767 and 0.796° for the *syn*-clinal and *anti*-clinal forms, respectively. The magnitude of the experimental value is given by

$$\tan 2\theta_R = 2F_{bc}/(B - C), \tag{3}$$

from which we obtain $\theta_R = 0.951°$. The sign of the experimental value of θ_R is indeterminate because F_{bc} depends on the relative phase of the tunneling wavefunctions. However, the dipole moment analysis described in the next section depends on the same phase choice. For the moment, it is sufficient to note the good agreement of the experimental and calculated values of θ_R for $\tau = 106.2°$.

VI. DIPOLE MOMENT ANALYSIS

The molecular electric dipole moment of the molecule was measured by studying the frequency shift as a function of the applied electric field for a number of the *M*

TABLE III

Observed *a*-Type and *b*-Type Rotational Transitions for $HOONO_2$ in the $v = 0$ and $v = 1$ Tunneling States of the First Excited NO_2 Torsional State (in MHz)

Transition	Measured Frequency v=0,1	Obs.-Calc.
5(3, 3) - 4(3, 2)	40733.530(60)a	0.022
5(3, 2) - 4(3, 1)	40963.490(40)	-0.012
7(0, 7) - 6(0, 6)	51217.970(50)	-0.055
8(1, 8) - 7(1, 7)	57569.605(47)	0.017
7(3, 4) - 6(3, 3)	58353.720(40)	0.000
11(0,11) - 10(1,10)	78043.185(38)	0.047
11(1,11) - 10(1,10)	78104.381(39)	0.024
11(0,11) - 10(0,10)	78161.628(35)	0.011
11(1,11) - 10(0,10)	78222.830(35)	-0.005
10(3, 8) - 9(3, 7)	81080.750(100)	-0.058
10(8, 3) - 9(8, 2)	81290.700(70)	0.011
10(7, 4) - 9(7, 3)	81418.210(50)	-0.034
10(6, 5) - 9(6, 4)	81616.186(54)	0.022
10(6, 4) - 9(6, 3)	81618.850(50)	-0.068
10(5, 6) - 9(5, 5)	81924.350(59)	-0.004
10(5, 5) - 9(5, 4)	81998.210(54)	-0.056
10(4, 7) - 9(4, 6)	82153.072(50)	0.014
10(4, 6) - 9(4, 5)	83163.564(58)	0.044
12(11, 1) - 11(11, 0)	97419.850(110)	-0.024
12(10, 2) - 11(10, 1)	97500.200(90)	0.001
12(9, 3) - 11(9, 2)	97607.920(70)	-0.009
12(8, 5) - 11(8, 4)	97758.530(70)	0.106
12(7, 6) - 11(7, 5)	97979.550(70)	0.037
12(7, 5) - 11(7, 4)	97980.330(70)	-0.050
12(6, 7) - 11(6, 6)	98318.510(70)	0.005
12(6, 6) - 11(6, 5)	98342.530(70)	0.010
14(0,14) - 13(1,13)	98521.930(100)	0.007
14(1,14) - 13(1,13)	98529.800(100)	0.034
14(0,14) - 13(0,13)	98537.630(90)	-0.010
13(1,12) - 12(1,11)	98613.310(100)	-0.014
14(2,13) - 13(2,12)	105061.820(40)	-0.037
14(1,13) - 13(1,12)	105304.140(40)	-0.079
15(0,15) - 14(1,14)	105328.700(50)	0.091
15(1,15) - 14(1,14)	105332.490(40)	-0.003
15(0,15) - 14(0,14)	105336.450(40)	-0.002
15(1,15) - 14(0,14)	105340.310(40)	-0.025
13(12, 2) - 12(12, 1)	105526.650(60)	-0.010
13(11, 2) - 12(11, 1)	105604.780(50)	-0.024
13(10, 4) - 12(10, 3)	105706.420(60)	-0.018
13(9, 4) - 12(9, 3)	105843.150(70)	0.009
13(8, 6) - 12(8, 5)	106034.780(60)	0.078
13(7, 7) - 12(7, 6)	106316.710(60)	-0.002
13(7, 6) - 12(7, 5)	106319.370(70)	-0.044
13(6, 8) - 12(6, 7)	106740.810(70)	0.017
13(6, 7) - 12(6, 6)	106800.770(70)	-0.004
13(5, 9) - 12(5, 8)	107207.200(60)	0.102
13(5, 8) - 12(5, 7)	107982.863(61)	-0.049
15(1,14) - 14(2,13)	111735.700(50)	0.100
15(2,14) - 14(2,13)	111898.037(33)	0.008
15(1,14) - 14(1,13)	112034.960(50)	-0.011
16(0,16) - 15(1,15)	112132.380(100)	0.033
16(1,16) - 15(1,15)	112134.243(43)	-0.014
16(0,16) - 15(0,15)	112136.159(47)	-0.071
16(1,16) - 15(0,15)	112138.100(100)	-0.040
13(3,10) - 12(3, 9)	112460.220(90)	-0.112
14(10, 5) - 13(10, 4)	113932.390(50)	0.048
14(9, 5) - 13(9, 4)	114103.040(50)	0.014
14(8, 6) - 13(8, 5)	114343.110(70)	-0.104
14(7, 8) - 13(7, 7)	114696.280(60)	-0.015
14(7, 7) - 13(7, 6)	114703.820(60)	-0.036
14(6, 9) - 13(6, 8)	115209.230(70)	0.044
14(6, 8) - 13(6, 7)	115346.410(80)	0.028
14(5,10) - 13(5, 9)	115638.004(68)	0.063
14(5, 9) - 13(5, 8)	117059.530(80)	-0.042
16(2,15) - 15(2,14)	118716.367(33)	0.000
16(1,15) - 15(1,14)	118792.040(30)	0.034

a) Uncertainties refer to the last digits given.

TABLE III—*Continued*

Transition	Measured Frequency v=0,1	Obs.-Calc.
17(0,17) - 16(1,16)	118934.530(50)	0.027
17(1,17) - 16(1,16)	118935.480(50)	0.041
17(0,17) - 16(0,16)	118936.370(50)	-0.043
17(1,17) - 16(0,16)	118937.330(40)	-0.019
15(2,13) - 14(2,12)	119677.210(90)	-0.203
5(5, 0) - 4(4, 0)	111469.730(100)	0.135
5(5, 1) - 4(4, 1)	111470.080(100)	-0.177
7(4, 4) - 6(3, 4)	112126.590(50)	0.029

components of several rotational transitions. Because of the perturbations caused by the similar energies of the two tunneling states in peroxynitric acid, some complications arise in calculating the Stark coefficients for the three dipole moment components of the ground state. Basically, the energy levels must be corrected to take into account the energy level perturbations. Since the analysis program employed here treats both states simultaneously, the appropriate coefficients for the transitions used in the analysis can be directly determined.

Because of the perturbations given in Eq. (2), *b*-dipole transitions are coupled with *c*-dipole transitions, while *a*-dipole transitions remain unmixed. Therefore a nominal *b*-dipole transition depends on both the *b*- and *c*-dipole moments in the following manner:

$$\langle J, K, 0|\mu_b|J', K', 0\rangle = \langle J, K, 0|\phi_b|J', K', 0\rangle\langle 0|\mu_b|0\rangle + \langle J, K, 0|\phi_c|J', K', 0\rangle\langle 0|\mu_c|1\rangle + \langle J, K, 0|\phi_b|J', K', 0\rangle\langle 1|\mu_b|1\rangle. \quad (4)$$

Since the second-order Stark effect depends on the square of Eq. (4), there will be a term dependent on the product $\mu_b\mu_c$ as well as the terms dependent on μ_b^2, μ_c^2, and μ_a^2. There is a fundamental indeterminacy in the sign of $\langle 0|\mu_c|1\rangle$ because of the indeterminate relative phases of the vibrational wavefunction. However, the product $\langle 0|\mu_b|0\rangle\langle 0|\mu_c|1\rangle\langle 0|F_{bc}|1\rangle$ is determinate because the sign is unaffected by the sign of the vibrational wavefunctions (as well as the signs of the *b* and *c* axes).

The frequency shifts of the 5_{33}–4_{32}, 5_{32}–4_{31}, and the 7_{07}–6_{06} *a*-type transitions for both components of the ground state lines were studied as a function of the applied electric field via Eq. (5):

$$\Delta\nu/E^2 = \sum_{i=a,b,c} (A_i + B_iM^2)\mu_i^2 + (A_{bc} + B_{bc}M^2)\mu_b\mu_c. \quad (5)$$

A total of nine M components were examined in order to obtain some statistical advantage for the determination of the three dipole moment components. The same transitions were also examined for the vibrational state, only in this case six M components were studied. The plate spacing of the absorption cell was calibrated using the $M = 2$ component of the $J = 3$–2 transition of OCS at 36488.814 MHz. The dipole moment of OCS employed was $\mu = 0.71519(3)$ D (*24*).

The results of the various fits are shown in Table VI. In the column labeled "Fit I" the results of the fit of all three dipole moment components along with the interaction

TABLE IV

Observed *c*-Type Rotational Transitions for $HOONO_2$ between the $v = 0$ and $v = 1$ Tunneling States of the HOO Torsional Ground and NO_2 Torsional States (in MHz)

Transition	v'-v"	Measured Frequency	Obs.-Calc.
Ground state of HOO torsion			
10(7, 4) - 10(6, 4)	0 - 1	100898.569(90)a	0.039
10(7, 3) - 10(6, 5)	0 - 1	100902.180(70)	-0.018
8(7, 1) - 8(6, 3)	0 - 1	101239.962(50)	-0.115
8(7, 2) - 8(6, 2)	0 - 1	101239.962(50)	0.070
7(7, 1) - 7(6, 1)	0 - 1	101339.600(60)	0.042
7(7, 0) - 7(6, 2)	0 - 1	101339.600(60)	0.016
11(7, 5) - 11(6, 5)	1 - 0	104151.800(80)	-0.038
11(7, 4) - 11(6, 6)	1 - 0	104164.280(100)	0.067
10(7, 4) - 10(6, 4)	1 - 0	104427.634(90)	0.019
10(7, 3) - 10(6, 5)	1 - 0	104431.264(90)	-0.020
8(7, 1) - 8(6, 3)	1 - 0	104780.284(46)	-0.112
8(7, 2) - 8(6, 2)	1 - 0	104780.284(46)	0.073
7(7, 1) - 7(6, 1)	1 - 0	104884.500(60)	0.003
7(7, 0) - 7(6, 2)	1 - 0	104884.500(60)	-0.024
22(8,15) - 22(7,15)	0 - 1	105232.303(30)	-0.004
5(5, 0) - 4(4, 0)	0 - 1	110221.612(38)	0.064
5(5, 1) - 4(4, 1)	0 - 1	110222.122(38)	-0.083
20(8,13) - 20(7,13)	0 - 1	110474.330(60)	-0.026
7(4, 4) - 6(3, 4)	0 - 1	110750.510(50)	-0.017
22(8,14) - 22(7,16)	0 - 1	110910.340(50)	-0.037
21(8,14) - 21(7,14)	1 - 0	111621.580(50)	0.157
17(8,10) - 17(7,10)	0 - 1	114234.600(40)	-0.053
22(8,14) - 22(7,16)	1 - 0	114273.320(40)	-0.003
17(8, 9) - 17(7,11)	0 - 1	114416.200(100)	0.062
19(5,14) - 19(4,16)	0 - 1	114768.450(40)	-0.033
21(8,13) - 21(7,15)	1 - 0	114819.200(50)	-0.021
16(8, 9) - 16(7, 9)	0 - 1	114955.080(50)	-0.066
16(8, 8) - 16(7,10)	0 - 1	115032.818(50)	0.100
15(8, 8) - 15(7, 8)	0 - 1	115523.487(41)	-0.030
19(8,12) - 19(7,12)	1 - 0	115549.860(50)	-0.258
15(8, 7) - 15(7, 9)	0 - 1	115554.470(40)	-0.014
20(8,12) - 20(7,14)	1 - 0	115566.990(50)	-0.029
9(1, 8) - 8(0, 8)	1 - 0	115680.000(100)	-0.349
10(2, 8) - 9(1, 8)	0 - 1	115726.330(40)	-0.068
14(8, 7) - 14(7, 7)	0 - 1	115974.580(80)	-0.059
14(8, 6) - 14(7, 8)	0 - 1	115986.120(40)	0.045
13(8, 6) - 13(7, 6)	0 - 1	116332.398(80)	-0.006
13(8, 5) - 13(7, 7)	0 - 1	116336.182(75)	-0.079
12(8, 5) - 12(7, 5)	0 - 1	116614.282(60)	0.121
12(8, 4) - 12(7, 6)	0 - 1	116615.250(60)	-0.078
11(8, 4) - 11(7, 4)	0 - 1	116833.450(50)	0.128
11(8, 3) - 11(7, 5)	0 - 1	116833.450(50)	-0.181
10(8, 3) - 10(7, 3)	0 - 1	117000.880(80)	0.040
10(8, 2) - 10(7, 4)	0 - 1	117000.880(80)	-0.030
16(8, 9) - 16(7, 9)	1 - 0	118433.581(50)	-0.021
16(8, 8) - 16(7,10)	1 - 0	118511.157(50)	-0.033
15(8, 8) - 15(7, 8)	1 - 0	119012.078(40)	-0.031
15(8, 7) - 15(7, 9)	1 - 0	119043.110(40)	0.019
14(8, 7) - 14(7, 7)	1 - 0	119472.600(50)	-0.026
14(8, 6) - 14(7, 8)	1 - 0	119484.130(50)	0.066
13(8, 6) - 13(7, 6)	1 - 0	119839.020(80)	0.011
13(8, 5) - 13(7, 7)	1 - 0	119842.900(80)	0.033
12(8, 5) - 12(7, 5)	1 - 0	120129.290(70)*	0.651
12(8, 4) - 12(7, 6)	1 - 0	120129.290(70)*	-0.516
20(4,16) - 19(5,14)	1 - 0	120142.730(50)	-0.097
11(8, 3) - 11(7, 5)	1 - 0	120355.110(50)*	-0.159
11(8, 4) - 11(7, 4)	1 - 0	120355.110(50)*	0.150
10(8, 3) - 10(7, 3)	1 - 0	120528.968(90)*	0.020
10(8, 2) - 10(7, 4)	1 - 0	120528.968(90)*	-0.050
9(8, 1) - 9(7, 3)	1 - 0	120659.890(50)	-0.034
9(8, 2) - 9(7, 2)	1 - 0	120659.890(50)	-0.022

a) Uncertainties refer to the last digits given. An asterisk after the frequency indicates blended lines. See the text for a discussion of the fitting of these blends.

TABLE IV—*Continued*

Transition	v'-v"	Measured Frequency	Obs.-Calc.
First Excited State of the NO_2 Torsion			
7(4, 3) - 6(3, 3)	0 - 1	110862.390(50)	-3.137
5(5, 0) - 4(4, 0)	0 - 1	110994.500(100)	-0.185
5(5, 1) - 4(4, 1)	0 - 1	110994.850(100)	-0.498
7(4, 4) - 6(3, 4)	0 - 1	111651.790(40)	0.143
5(5, 0) - 4(4, 0)	1 - 0	111944.950(100)	0.441
5(5, 1) - 4(4, 1)	1 - 0	111945.300(100)	0.129
7(4, 4) - 6(3, 4)	1 - 0	112601.380(50)	-0.091

term $2\mu_b\mu_c$ are shown. Although the interaction term appears to be marginally statistically determined, the absolute magnitude is unrealistic (obviously it should be $\sim 0.8 = \mu_b\mu_c$). In order to alleviate the situation, a nonlinear least-squares approach was tried. The interaction term was fixed using the values of μ_b and μ_c as determined from Fit I. Equation (5) was rearranged by subtracting the frequency shift due to the interaction term as determined from the values of μ_b and μ_c of the previous iteration. The values for the three dipole moment components were then redetermined. The columns labeled "Fit II" and "Fit III" give the results after two such iterations. Note that two sets of values are required because the sign on the interaction term is not established. Fit II assumes a minus sign and Fit III assumes a plus sign. Both results

TABLE V

Spectroscopic Constants for Peroxynitric Acid in the Ground and First Excited NO_2 Torsional States

	Ground State		Vibrational State	
A_0	11994.4997(68)[a]	MHz	11935.939(20)	MHz
A_1	11994.3029(56)	MHz	-	
B_0	4665.2445(22)	MHz	4663.2762(26)	MHz
B_1	4665.0080(30)	MHz	-	
C_0	3397.1888(31)	MHz	3401.9196(12)	MHz
C_1	3397.1563(31)	MHz	-	
D_{J0}	1.4255(38)	kHz	1.4029361(54)	kHz
D_{J1}	1.4138(29)	kHz	-	
D_{JK0}	5.365(13)	kHz	5.747685(20)	kHz
D_{JK1}	5.396(11)	kHz	-	
D_{K0}	5.695(66)	kHz	19.14771(60)	kHz
D_{K1}	5.606(56)	kHz	-	
δ_{J0}	0.3616(24)	kHz	0.3542744(29)	kHz
δ_{J1}	0.3540(30)	kHz	-	
δ_{K0}	4.334(63)	kHz	3.889247(59)	kHz
δ_{K1}	4.130(46)	kHz	-	
E_1	1782.636(97)	MHz	474.9(4)	MHz
F_{01}	21.058(10)	MHz	-	

[a] The numbers in parentheses represent one standard deviation of the number.

TABLE VI

Dipole Moment Analysis for the Ground and First Excited NO_2 Torsional States of Peroxynitric Acid

	Ground State			Vibrational State
	Fit I[a]	Fit II[b]	Fit III[b]	
μ_a	1.173(6)	1.185(6)	1.187(6)	1.179(5)
μ_b	0.70(13)	0.94(3)	0.97(9)	0.53(12)
μ_c	1.157(33)	1.288(2)	1.304(2)	1.288(6)
$\mu_b\mu_c$	-20.8(47)	(-)	(+)	-

[a]Fit I is an independent fit of all three dipole moment components and the $\mu_b\mu_c$ interaction term. Unfortunately the magnitude is unreasonable as it should be ~0.81 (i.e., $\mu_b{\cdot}\mu_c$).

[b])Fits II and III are the results of two iterations of fixing the interaction term at the values obtained from $\mu_b{\cdot}\mu_c$. Fit II assumes a(-) sign and Fit III assumes a(+) sign.

are similar, which indicates that the transitions chosen for the analysis do not have a strong dependence on the interaction term. The preferred fit, however, is the one with the (−) sign on the interaction term since the sign agrees with that obtained from Fit I and the standard deviation on μ_b is three times smaller than the one which assumes a (+) sign on the interaction term. The dipole moments for the vibrational state are shown in the last column of the table.

The value for μ_b can be determined independently from relative intensity measurements. All that is needed for this determination is to find a region where *a*- and *b*-type transitions occur relatively close together. For a slightly asymmetric prolate rotor-like peroxynitric acid, the regions of intermediate J and $K_{-1} = 0$ and 1 provide just such a situation. The $J + 1_{0,J+1}$–$J_{0,J}$ and the $J + 1_{1,J+1}$–$J_{1,J}$ *a*-type, *R*-branch transitions occur in close proximity to the $J + 1_{0,J+1}$–$J_{1,J}$ and the $J + 1_{1,J+1}$–$J_{0,J}$ *b*-type transitions. Accordingly, the relative intensities of the J = 14–13, 15–14, 16–15, and the 17–16 sets of these transitions were measured for both the ground state and the vibrational state. Then using the predetermined values of μ_a from Table VI, values for μ_b were calculated. The average of three sets of intensity measurements for each state yielded 0.772(15) and 0.686(12) D for μ_b of the ground and excited vibrational states, respectively. It is reassuring that the values fall in between the values determined for the two states in the normal Stark effect analysis. Furthermore, the value for the vibrational state is slightly smaller than the ground state as was also found in the first analysis. Evidently, the NO_2 torsional motion leads to a configuration in which μ_b is smaller.

In order to see if the dipole moments could be used for the determination of which clinal conformer was being observed, a simple bond moment calculation was made for nitric acid, hydrogen peroxide, and peroxynitric acid. The bond moments used were from Smyth (*25*) and are shown in Table VII. The results of these calculations and the experimental values are also shown in Table VII. From the excellent agreement obtained for nitric acid and hydrogen peroxide, one would expect that a similar estimation for peroxynitric acid would be fairly good. For $HOONO_2$ the estimation was

TABLE VII

Calculated[a] and Observed Dipole Moments for HOOH, HNO_3, and $HOONO_2$

Dipole Component	HOOH		HNO_3	
	calc.	obs.[b]	calc.	obs.[c]
μ_a	-	-	2.09	1.99
μ_b	1.48	1.58	0.90	0.88
μ_c	-	-	-	-

$HOONO_2$

	syn-clinal 72°	anti-clinal 106°	
	calc.	calc.	obs.
μ_a	1.1	1.6	1.187(6)
μ_b	0.3	1.0	0.94(3)
μ_c	1.4	1.4	1.288(2)

[a]Using the following bond moments H-O = 1.51D., N-O = 0.3D, N=O = 2.0D from Reference #27.

[b]Reference #26.

[c]Reference #11.

made using the three parameters that were determined from the structural fit as discussed earlier along with the remainder of the parameters from the nitric acid and hydrogen peroxide structures (see Table I). The comparisons are fairly good especially for μ_b and μ_c for the *anti*-clinal forms (106°). Note especially that while the calculated value of $\mu_b\mu_c$ is negative for both forms, the calculated value of $\mu_b\mu_c F_{bc}$ is negative for the *anti*-clinal form and positive for the *syn*-clinal form. The experimental preference for a negative sign is therefore consistent with the *anti*-clinal form.

VII. COMPARISON WITH THEORETICAL STRUCTURE

During the course of this work, we became aware of a theoretical paper in which the geometry of the lowest energy conformer was investigated for peroxynitric acid (*27*). In that work, the minimum energy configuration was determined using several different basis sets. The lowest energy structure was one in which the dihedral angle (α) between the $N_4O_3O_2$ and $O_6N_4O_5$ planes was 23.9°. The dihedral angle (τ) between the HO_2O_3 and the NO_2 planes was determined to be 102.9°. A detailed comparison of all the molecular parameters is not warranted, however, it is interesting to compare the two dihedral angles. From the microwave work, we can say with certainty that $\alpha = 0$. The other angle, τ, is the one with which we have the dichotomy, since we can fit the rotational constants to either a ~72° *syn*-clinal form or a ~106° *anti*-clinal form. The dipole moment analysis tends to favor the *anti*-clinal form which is in agreement with the theoretical work.

VIII. ESTIMATION OF THE VIBRATIONAL STATE ENERGY

The difference in energies of the ground state and the lowest vibrational state (NO_2 torsion) can be determined by measuring the relative intensities of two transitions (*28*,

13). For the case of peroxynitric acid the procedure is quite simple and should provide a fairly reliable estimate of the energy difference. As can be seen in Fig. 2, one can compare the relative intensities of the sum of the resolved doublet (ground state) and the degenerate doublet (NO_2 torsion). Relative intensity measurements on 16 transitions similar to the ones shown in Fig. 2 have been made and the average ratio found to be 2.030(61), where the number in parentheses represents 1 SD. For this case the intensity ratio reduces to a simple Boltzmann relationship as given by Eq. (6) (*13*):

$$I_{gs}/I_{vib} = e^{-(E_{gs}-E_{vib})/kT} \tag{6}$$

where k is the Boltzmann constant, T is the temperature, I_{gs}/I_{vib} is the ratio determined above and $E_{gs} = 0$ is the energy of the ground state. At room temperature (295 K) this gives $E_{vib} = 145(6)\ cm^{-1}$.

IX. DISCUSSION

In addition to the structural determination and the dipole moment measurements that we obtained, one of the goals in the study was to ascertain the difficulties which might be encountered in a high-resolution infrared analysis. The observed ground state rotational constants would provide a distinct advantage in assignments and analysis since then only the upper state constants would be uncertain. As can be seen from the microwave study described here, the infrared analysis will be complicated by the perturbations and the tunneling motion in the ground state. Since the magnitudes of the splittings caused by the tunneling are fairly small (usually about 10 MHz or less), one might expect to see a broadening of the infrared lines as opposed to splittings. However, the magnitude of the splittings in an excited vibrational state cannot be predicted a priori. If the splitting decreases, as we found for the low-frequency NO_2 torsion, it would make the IR spectrum less complicated. Another complicating factor is the fact that, in the ground state, numerous perturbations are observed due to Coriolis interactions. If the vibrational excited states exhibit similar or somewhat larger splittings, the vibrational bands may exhibit numerous perturbations that would make the analysis extremely difficult. Perhaps the most fruitful region to begin an infrared analysis would be in the far infrared where the NO_2 torsion occurs since for this vibration, rotational constants for both the upper and lower states are known from this work.

ACKNOWLEDGMENT

Portions of this work were performed at the Jet Propulsion Laboratory, California Institute of Technology, under contract with the National Aeronautics and Space Administration.

RECEIVED: September 12, 1985

REFERENCES

1. H. E. G. SINGBEIL, W. D. ANDERSON, R. W. DAVIS, M. C. L. GERRY, E. A. COHEN, H. M. PICKETT, F. J. LOVAS, AND R. D. SUENRAM, *J. Mol. Spectrosc.* **103,** 466–485 (1984).
2. R. D. SUENRAM AND F. J. LOVAS, *J. Mol. Spectrosc.* **105,** 351–359 (1984).
3. H. NIKI, P. D. MAKER, C. M. SAVAGE, AND L. P. BREITENBACH, *Chem. Phys. Lett.* **45,** 564–566 (1977).

4. S. Z. LEVINE, W. M. USELMAN, W. H. CHAN, J. G. CALVERT, AND J. H. SHAW, *Chem. Phys. Lett.* **48,** 528–535 (1977).
5. C. J. HOWARD, *J. Chem. Phys.* **67,** 5258–5263 (1977).
6. R. A. GRAHAM, A. M. WINER, AND J. N. PITTS, JR., *J. Chem. Phys.* **68,** 4505–4510 (1978).
7. R. A. KENLEY, P. L. TREVOR, AND B. Y. LAN, *J. Amer. Chem. Soc.* **103,** 2203–2206 (1981).
8. N. D. SZE AND M. K. W. KO, *Atmos. Environ.* **15,** 1301–1307 (1981).
9. R. D. SUENRAM AND F. J. LOVAS, *J. Amer. Chem. Soc.* **102,** 7180–7184 (1980).
10. D. R. JOHNSON AND R. PEARSON, JR., "Methods of Experimental Physics," Vol. 13, Part B, pp. 102–134, Academic Press, New York, 1976.
11. P. N. GHOSH, C. E. BLOM, AND A. BAUDER, *J. Mol. Spectrosc.* **89,** 159–173 (1981).
12. W. B. DIXON AND E. B. WILSON, JR., *J. Chem. Phys.* **35,** 191–198 (1961).
13. D. G. SCROGGIN, J. M. RIVEROS, AND E. B. WILSON, *J. Chem. Phys.* **60,** 1376–1385 (1974).
14. G. A. KHACHKURUZOV AND I. N. PRZHEVALSKII, *Opt. Spektrosk.* **36,** 299–303 (1974).
15. M. OLDANI, T. K. HA, AND A. BAUDER, *J. Amer. Chem. Soc.* **105,** 360–365 (1983).
16. J. A. CUGLEY, W. BOSSERT, A. BAUDER, AND HS. H. GÜNTHARD, *Chem. Phys.* **16,** 229–235 (1976).
17. R. H. MILLER, D. L. BERNITT, AND I. C. HISATUNE, *Spectrochima Acta* **23A,** 223–236 (1967).
18. J. K. G. WATSON, *J. Chem. Phys.* **46,** 1935–1949 (1967).
19. W. H. KIRCHHOFF, *J. Mol. Spectrosc.* **41,** 333–380 (1972).
20. H. M. PICKETT, *J. Chem. Phys.* **56,** 1715–1723 (1972).
21. W. KLYNE AND V. PRELOG, *Experimentia* **16,** 521–523 (1960).
22. R. H. SCHWENDEMAN, *in* "Critical Evaluation of Chemical and Physical Structural Information" (D. R. Lide, Jr., and M. A. Paul, Eds.), pp. 94–115, National Academy of Sciences–National Research Council, Washington, D. C., 1974.
23. J. M. L. J. REINHARTZ AND A. DYMANUS, *Chem. Phys. Lett.* **24,** 346–351 (1974).
24. C. H. TOWNES AND A. L. SCHAWLOW, "Microwave Spectroscopy," pp. 248–283, McGraw-Hill, New York, 1955.
25. C. P. SMYTH, "Dielectric Behavior and Structure," pp. 244–245, McGraw-Hill, New York, 1955.
26. E. A. COHEN AND H. M. PICKETT, *J. Mol. Spectrosc.* **87,** 582–583 (1981).
27. R. P. SAXON AND B. LIU, *J. Phys. Chem.* **89,** 1227–1232 (1985).
28. Ref. (*24*), p. 101, Eq. (4-28).